
This copy is for your personal, non-commercial use only.

If you wish to distribute this article to others, you can order high-quality copies for your colleagues, clients, or customers by [clicking here](#).

Permission to republish or repurpose articles or portions of articles can be obtained by following the guidelines [here](#).

The following resources related to this article are available online at www.sciencemag.org (this information is current as of October 24, 2011):

Updated information and services, including high-resolution figures, can be found in the online version of this article at:

<http://www.sciencemag.org/content/334/6054/347.full.html>

Supporting Online Material can be found at:

<http://www.sciencemag.org/content/suppl/2011/09/08/science.1203580.DC1.html>

A list of selected additional articles on the Science Web sites **related to this article** can be found at:

<http://www.sciencemag.org/content/334/6054/347.full.html#related>

This article **cites 33 articles**, 7 of which can be accessed free:

<http://www.sciencemag.org/content/334/6054/347.full.html#ref-list-1>

800,000 Years of Abrupt Climate Variability

Stephen Barker,^{1*} Gregor Knorr,² R. Lawrence Edwards,³ Frédéric Parrenin,^{4,5} Aaron E. Putnam,⁶ Luke C. Skinner,⁷ Eric Wolff,⁸ Martin Ziegler¹

We constructed an 800,000-year synthetic record of Greenland climate variability based on the thermal bipolar seesaw model. Our Greenland analog reproduces much of the variability seen in the Greenland ice cores over the past 100,000 years. The synthetic record shows strong similarity with the absolutely dated speleothem record from China, allowing us to place ice core records within an absolute timeframe for the past 400,000 years. Hence, it provides both a stratigraphic reference and a conceptual basis for assessing the long-term evolution of millennial-scale variability and its potential role in climate change at longer time scales. Indeed, we provide evidence for a ubiquitous association between bipolar seesaw oscillations and glacial terminations throughout the Middle to Late Pleistocene.

Ice core records from Greenland first demonstrated the existence of repeated, large, abrupt shifts in Northern Hemisphere climate during the last ice age (1, 2). These shifts are one expression of a global system that is capable of driving major changes in climate components such as ocean temperatures (3, 4) and monsoon rainfall (5). The Greenland records provide an archetypal view of abrupt climate variability (6) over the last glacial cycle, which was characterized by rapid alternations between cold (stadial) and warmer (interstadial) conditions [known as Dansgaard-Oeschger (D-O) oscillations]. But ironically, the very high temporal resolution of these records makes it difficult to look farther back in time; the high accumulation rates on the Greenland ice sheet mean that more than 3000 m of ice may represent just 100,000 years of climate history. Fortunately, climate records preserved in Antarctic ice (7) enable us to address this fundamental problem.

The thermal bipolar seesaw model (8, 9) attempts to explain the observed relationship between millennial-scale temperature variability observed in Greenland and Antarctica by calling on variations in the strength of the Atlantic meridional overturning circulation (AMOC). The northward heat transport associated with this circulation (10) implies that changes in the strength of overturning should lead to opposing temperature responses in either hemisphere. According to the seesaw model, a transition from weak to strong AMOC would cause an abrupt warming across the

North Atlantic region (a D-O warming event) while temperatures across Antarctica would (in general) shift from warming to cooling. The ocean-atmosphere climate system is an integrated and synergistic system, and it is important to note that the overall concept of the bipolar seesaw we invoke here is not restricted to oceanic processes but also includes atmospheric shifts that may be related to the variations we are interested in (9, 11–14).

According to the thermal bipolar seesaw model, we should observe an antiphase relationship between the Greenland temperature anomaly and the rate of change of Antarctic temperature (9). This can be illustrated by a lead/lag analysis of the methane-tuned temperature records after removal of their orbital time scale variability (6) (Greenland, GL_T _hi, and Antarctica, AA_T _hi) and the first time derivative of Antarctic temperature, AA_T _hi' (Fig. 1). Comparison of the undifferentiated records illustrates the historical debate as to whether the two signals are positively correlated, with a southern lead of 1000 to 1600 years, or negatively correlated, with the north leading by 400 to 800 years (15, 16). However, as implied in (9) and illustrated in Fig. 1, a near zero-phase anticorrelation is observed between GL_T _hi and AA_T _hi' (Fig. 1). Uncertainties in the ice age–gas age offset (Δ age), which may be up to hundreds of years (17), mean that an exact antiphase relationship is unlikely to be observed (6). As described by (18) using a similar approach, the process of differentiating amplifies noise in the original temperature record. Smoothing the record of AA_T _hi before differentiating reduces this noise but will compromise the ability of AA_T _hi' to replicate the abrupt nature of D-O warming events and reduce the predicted amplitude of smaller events. The choice of smoothing window is therefore a trade-off between these effects (6) (Fig. 1).

The empirical relations illustrated in Fig. 1 offer the possibility of producing a synthetic record of Greenland climate using the Antarctic record, with the purpose of reconstructing the nature of northern variability beyond the present limit of the Greenland records. The record of Green-

land temperature (GL_T) is broken down into its orbital and millennial time scale components, GL_T _lo and GL_T _hi, respectively (Fig. 2 and fig. S5), where GL_T _lo is a 7000-year smoothing of GL_T (6) and GL_T _hi is the difference between GL_T and GL_T _lo. We consider GL_T _hi as the northern temperature anomaly with respect to mean background conditions. Building on Fig. 1, we assume that the rate of Antarctic temperature change is inversely proportional to the northern temperature anomaly. We therefore scale the amplitude of AA_T _hi' to match that of GL_T _hi to produce a synthetic record of northern millennial-scale temperature variability, GL_T _syn_hi (Fig. 2C) (6). It can be seen that a synthetic reconstruction of GL_T could be made by combining GL_T _syn_hi with an estimate for GL_T _lo. The orbital time scale components of the Greenland and Antarctic temperature records (GL_T _lo and AA_T _lo, respectively) are highly correlated, with the southern record leading the north by ~2000 years (6). We therefore incorporate longer time scale variations into our reconstruction by substituting GL_T _lo with a scaled version of AA_T _lo, shifted by 2000 years (which we call GL_T _syn_lo) (fig. S5) (6). Our full reconstruction, GL_T _syn (Fig. 2D), is then the sum of GL_T _syn_lo and GL_T _syn_hi.

Our formulation of the thermal bipolar seesaw concept is qualitatively analogous to that of (9) in that it implies the existence of a heat reservoir that convolves the northern signal, producing a southern signal with a longer characteristic time scale. Our approach is slightly different in that we relate the rate of Antarctic temperature change directly to the northern temperature anomaly. Indeed, we note that for some long stadial events, particularly those associated with glacial terminations, Antarctic temperatures appear to rise unabated until an abrupt warming event occurs in the north (19). On the other hand, our formulation does not imply that Antarctic temperatures must continue to rise indefinitely whenever Greenland is cold, only while it is cold with respect to background conditions (defined by the orbital time scale component). We also note that northern temperature (regardless of background conditions) is not always constant throughout stadial events. For example, Greenland warmed significantly during cold stadial 21 (Fig. 2D). By our formulation, the rate of Antarctic temperature rise during this event would decrease correspondingly, in line with observations (Fig. 2A) (20).

We used a thresholding approach for predicting the occurrence of abrupt Greenland warming events based on minima in the second time differential of AA_T (AA_T'') (Fig. 2, E and F). This has an advantage over use of the first differential (decreasing through zero) because it is capable of distinguishing between events of varying magnitude and incorporates information about conditions before and after an abrupt event (6). Using a relatively insensitive threshold (blue dashed line in Fig. 2F), we are able to identify the largest D-O

¹School of Earth and Ocean Sciences, Cardiff University, Cardiff CF10 3AT, UK.

²Alfred Wegener Institute, 27570 Bremerhaven, Germany.

³Department of Earth Sciences, University of Minnesota, Minneapolis, MN 55455, USA.

⁴Laboratoire de Glaciologie, CNRS and Joseph Fourier University, 38400 Grenoble, France.

⁵Laboratoire Chrono-Environnement, 25000 Besançon, France.

⁶Department of Earth Sciences and Climate Change Institute, University of Maine, Orono, ME 04469, USA.

⁷Godwin Laboratory for Palaeoclimate Research, Department of Earth Sciences, University of Cambridge, Cambridge CB2 3EQ, UK.

⁸British Antarctic Survey, Madingley Road, High Cross, Cambridge CB3 0ET, UK.

*To whom correspondence should be addressed. E-mail: barkers3@cf.ac.uk

temperature shifts recorded in Greenland, whereas “smaller” events, such as D-O 2, require a more sensitive threshold (red line). Accordingly, we are able to identify almost all of the canonical D-O events over the past 90,000 years without introducing “spurious events.” We incorporate a correction, based on the time integrated per 55-cm sample of ice (7), to account for loss of temporal resolution in the deeper parts of the ice core (6).

Our synthetic reconstruction of Greenland temperature closely resembles the observed record in terms of both its timing and the structure of individual events (Fig. 2). This is despite probable variability in the relationships between $\delta^{18}\text{O}$ [for the Greenland Ice Sheet Project 2 ice core (GISP2)] or δD [for the European Project for Ice Coring in Antarctica Dome C ice core (EDC)] versus local temperature through time (21) and other millennial-scale variability that might not be related to the bipolar seesaw. We find similar results using alternative Antarctic ice core records (6). On the basis of the predictive ability of $\text{GL}_{\text{T_hi}}$ over the past ~100,000 years, we can extend our reconstruction back to ~800,000 years ago (Fig. 3 and Fig. 4). In doing so we implicitly assume that the empirical relationships observed over

the last glacial cycle held during earlier periods. Given the inherent uncertainty in this assumption, we do not claim particular skill at predicting the absolute amplitude of earlier events; however, we do suggest that to the extent that the underlying physical mechanisms did persist throughout the past 800,000 years, the timing and overall structure of events will be relatively robust.

To test this hypothesis, we compared our synthetic reconstructions with real climate records. The record of Asian monsoon variability derived from cave deposits (speleothems) in China (5, 22) is one of the best candidates for this task (Fig. 3). The Chinese speleothem $\delta^{18}\text{O}$ record is thought to represent changes in the proportion of low $\delta^{18}\text{O}$ (summer monsoon) rainfall within annual totals (22) and can be considered a measure of the amount of summer monsoon rainfall or monsoon intensity. The combined record from several deposits taken from a number of caves provides a continuous, absolutely dated record over the past ~400,000 years (22). The record is dominated by orbital time scale changes, possibly related to the influence of boreal summer insolation on the strength of the Asian monsoon (6). Re-

moval of this variability by normalizing to the insolation curve (6) reveals distinctive millennial time scale activity that has been shown to correspond with D-O variability over Greenland during the last glacial cycle (5, 22). This correspondence is thought to be caused by latitudinal shifts in the position of the Intertropical Convergence Zone (ITCZ) and related atmospheric phenomena in response to variations in the AMOC and related changes in North Atlantic temperature (11).

There is a strong one-to-one correspondence between inferred weak-monsoon events and our reconstructed cold events in Greenland (Fig. 3). Moreover, there are pronounced similarities in the structure of abrupt events, particularly during deglacial episodes (terminations); the multiple weak-monsoon events associated with glacial terminations of the Late Pleistocene (22) are reflected by multiple cold events in our records. Our reconstruction suggests the occurrence of large-amplitude “D-O-type” oscillations between 160,000 and 180,000 years ago [during marine isotope stage 6 (MIS 6)] (Fig. 3). These may be compared with similar events in the records of planktonic $\delta^{18}\text{O}$ and tree pollen from a marine

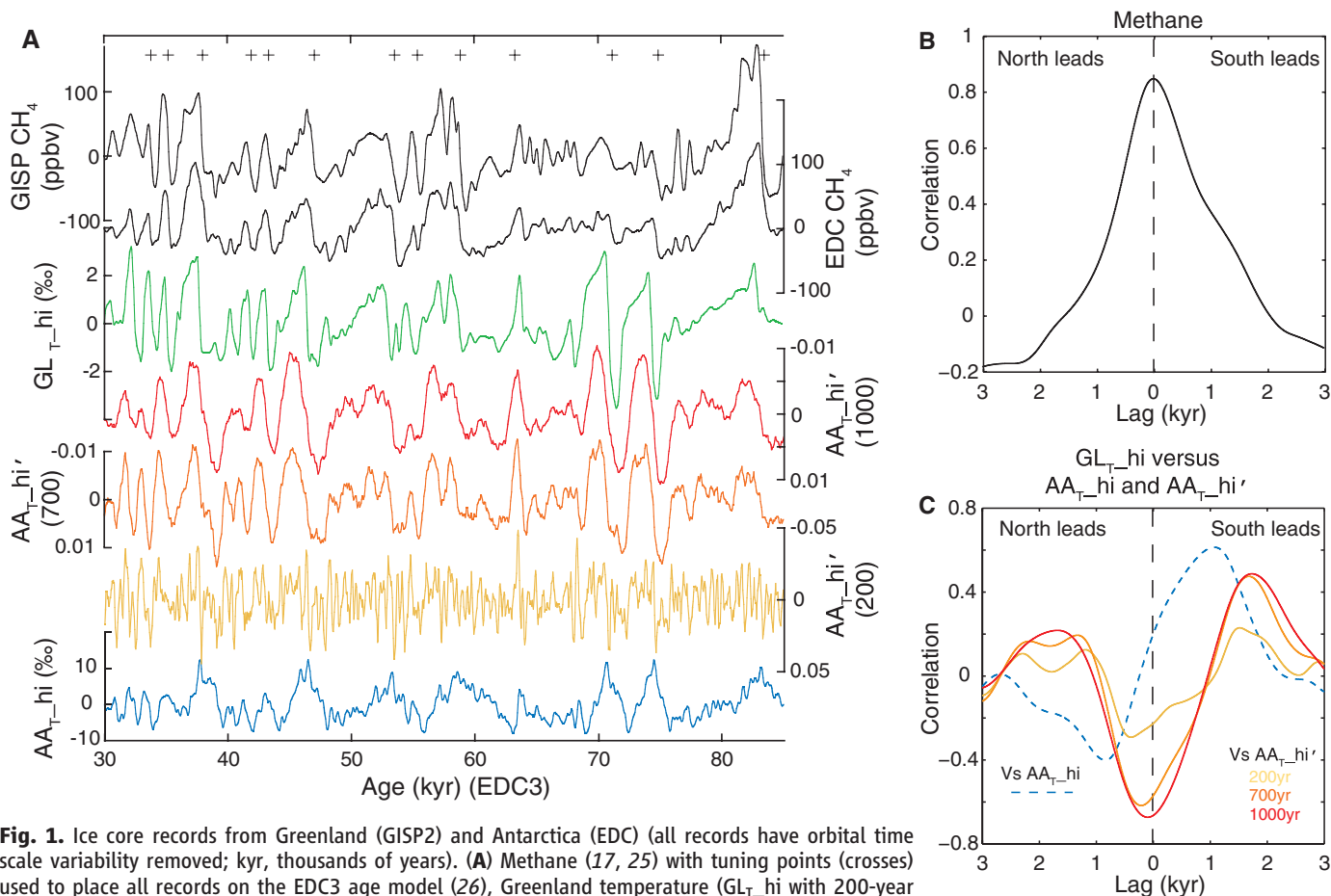


Fig. 1. Ice core records from Greenland (GISP2) and Antarctica (EDC) (all records have orbital time scale variability removed; kyr, thousands of years). **(A)** Methane (17, 25) with tuning points (crosses) used to place all records on the EDC3 age model (26), Greenland temperature ($\text{GL}_{\text{T_hi}}$ with 200-year smoothing) derived from $\delta^{18}\text{O}$ of ice (2), and Antarctic temperature ($\text{AA}_{\text{T_hi}}$, 200-year smoothing) from δD of ice (7). First derivatives of $\text{AA}_{\text{T_hi}}$ ($\text{AA}_{\text{T_hi}'}$) are shown for various smoothing lengths (in brackets) of the undifferentiated record. **(B)** Lead/lag correlation of the methane records suggests successful tuning of the gas records. **(C)** Lead/lag correlations between $\text{GL}_{\text{T_hi}}$, $\text{AA}_{\text{T_hi}}$, and $\text{AA}_{\text{T_hi}'}$ reveal the well-known relation between northern and southern temperature records and the antiphase relationship between $\text{GL}_{\text{T_hi}}$ and $\text{AA}_{\text{T_hi}'}$.

Fig. 2. Reconstructing millennial-scale climate variability over Greenland using the Antarctic temperature record. **(A)** The record of δD from the EDC ice core (AA_T) (7) with a 7000-year smoothing of the same record (AA_{T_lo}). **(B)** Removal of orbital time scale variability and application of a 700-year smoothing (6) produces AA_{T_hi} . **(C)** AA_{T_hi} is differentiated and then scaled to GL_{T_hi} (green curve) to produce $GL_{T_syn_hi}$ (orange curve). **(D)** A synthetic reconstruction of Greenland temperature variability (GL_{T_syn} ; red curve) constructed by adding $GL_{T_syn_hi}$ to $GL_{T_syn_lo}$ (6). Green curve is GISP2 $\delta^{18}O$ placed on EDC3 via methane tuning (Fig. 1). **(E and F)** Minima in $AA_{T''}$ below a threshold (dashed lines) are used to predict the occurrence of major warming events in Greenland **(F)**, identified by the corresponding colored dots in **(E)**. A threshold value of -1.2×10^{-5} (red dashed line and dots) has good success at picking canonical D-O events [green numbers in **(D)** and **(E)**] without introducing spurious events.

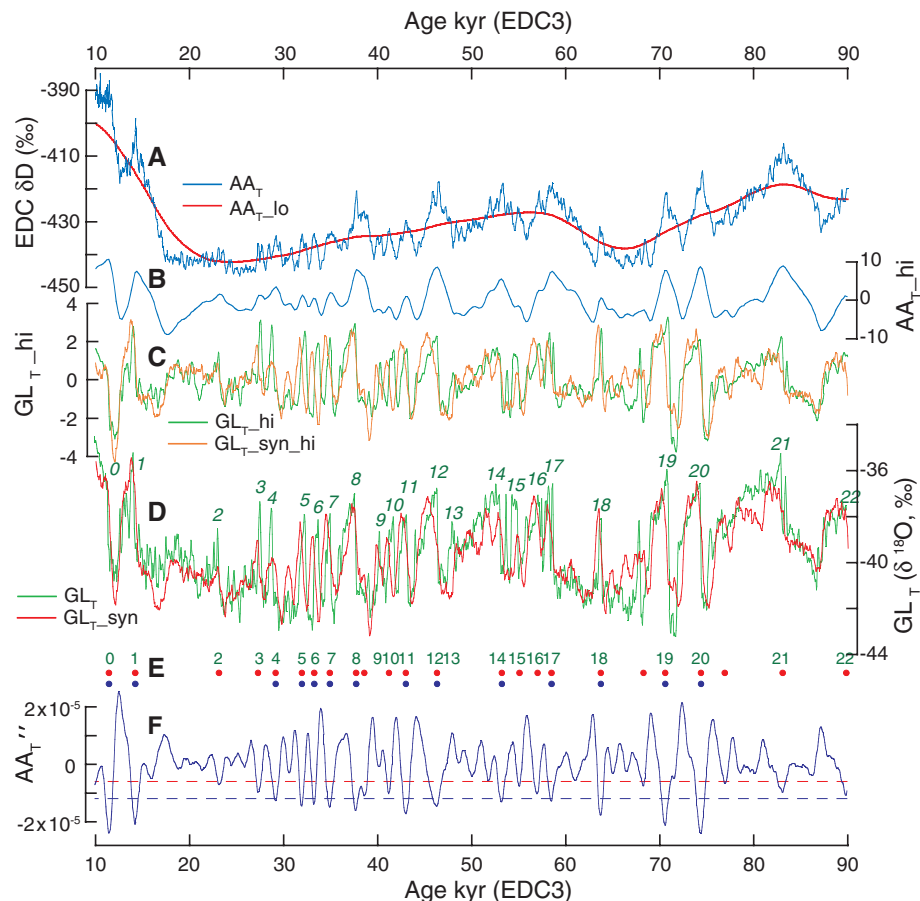
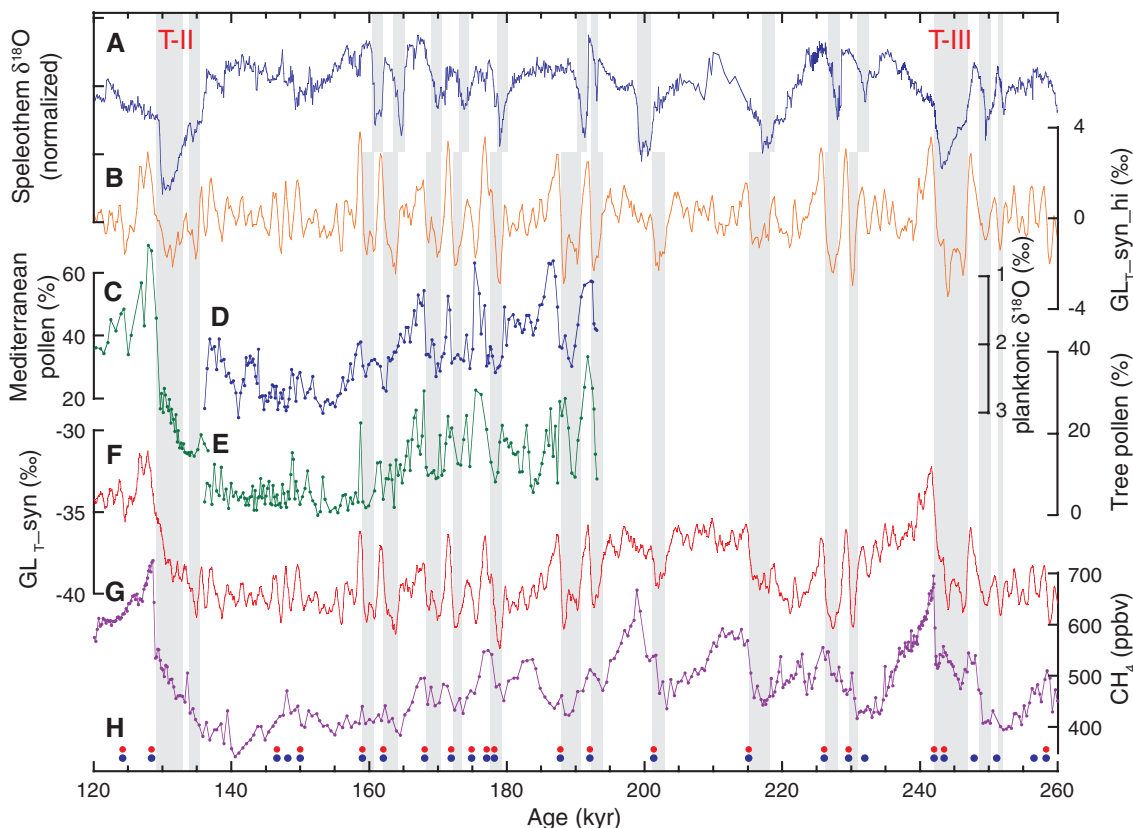


Fig. 3. **(A to H)** Comparison of reconstructed Greenland climate variability with other records. The normalized record of monsoon variability from China **(A)** (5, 22), marine records from the Iberian Margin [**(C)** to **(E)**] (23, 32), and the record of atmospheric CH_4 **(G)** (25) share many features in common with our records derived from the Antarctic temperature record [**(B)** and **(F)**]. Colored dots in **(H)** represent the occurrence of D-O events predicted from $AA_{T''}$ using a fixed (red) or variable (blue) threshold (6). All records are on the EDC3 time scale (26) except the monsoon record which is on its own absolute time scale (22). The pollen record from MD95-2042 (32) **(C)** was placed on EDC3 by tuning the corresponding planktonic $\delta^{18}O$ record (24) to GL_{T_recon} . Gray bars indicate cold conditions and periods of weak monsoon. Glacial terminations are indicated by Roman numerals.



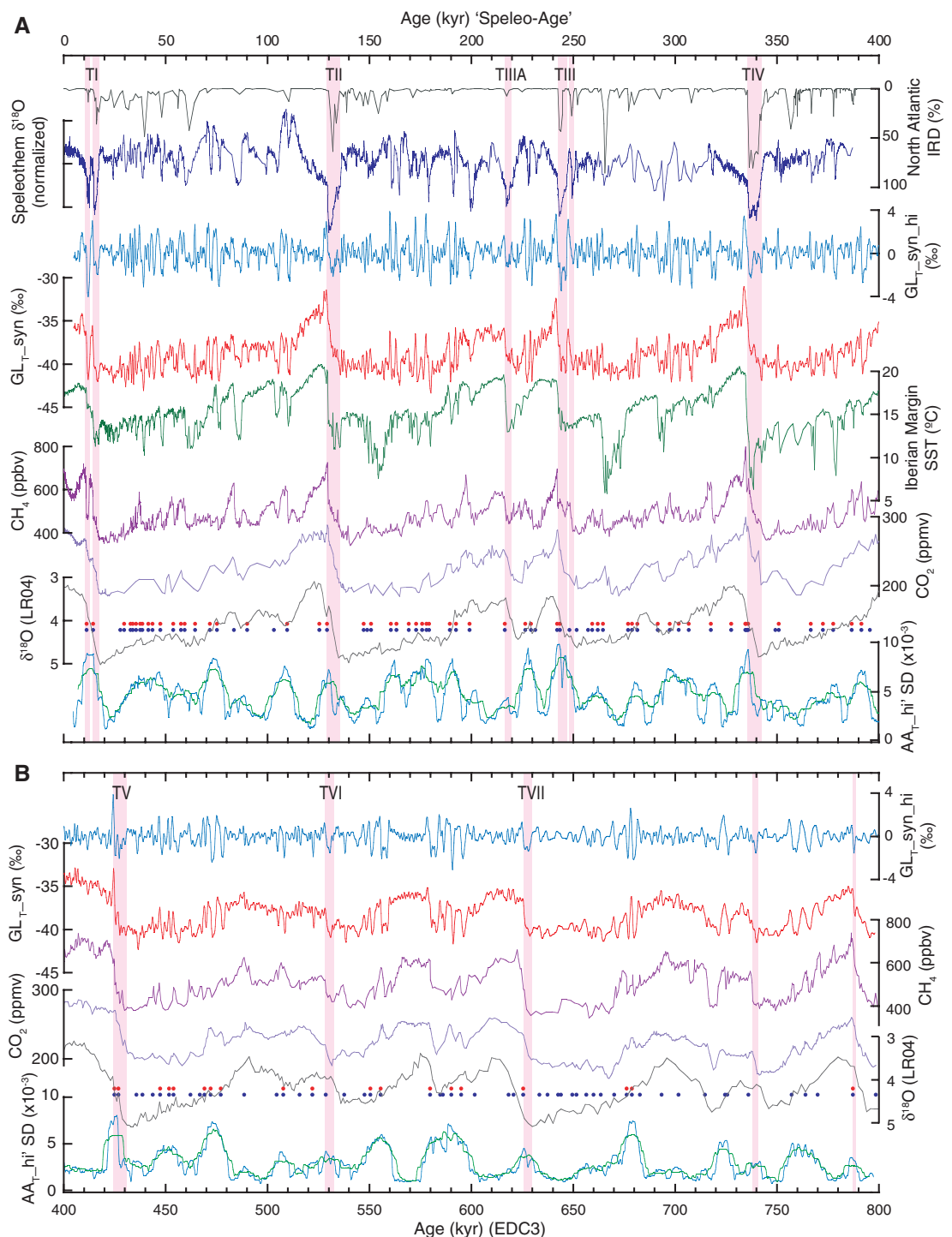
sediment core taken from the Iberian Margin (23). On the basis of the findings of Shackleton *et al.* (24), the Iberian Margin records were tuned to the EDC δD record via the record of benthic $\delta^{18}O$ from the same core (23). The tuning exercise did not involve the surface records, which therefore provide a quasi-objective “target” for comparing with our reconstruction [which should be aligned with the surface-ocean records according to (24)], and there is good agreement in the timing and structure of the abrupt events during

MIS 6. We also note good agreement between our reconstructions and the record of atmospheric CH_4 (25). Our predicted D-O warming events are generally aligned with sharp increases in CH_4 (similar to the observed relationship during MIS 3). This relationship holds for the entire 800,000-year record (Fig. 4) and provides critical ground-truthing for our reconstruction.

Building on previous studies (22), we used the precise and absolutely dated Chinese speleothem record to place our reconstruction on an

absolute time scale for the past 400,000 years. We did this by aligning the cold events in our reconstruction with the inferred weak-monsoon events in the speleothem record (Fig. 4) (6). The EDC3 age scale (which remains the fundamental basis for our model) was derived through a combination of ice flow modeling and various age markers, including orbital tuning constraints (26). By tuning the millennial-scale features of GL_{T_syn} to the speleothem record, we provide a refinement of the age scale that provides an

Fig. 4. (A and B) 800,000 years of abrupt climate variability. Records of North Atlantic IRD (4), monsoon rainfall (5, 22) (normalized) and SST from the Iberian Margin (27) all show strong similarities with our reconstruction of Greenland climate variability ($GL_{T_syn_hi}$ and GL_{T_syn}). Glacial terminations (identified by Roman numerals) are characterized by cold conditions across Greenland and the North Atlantic and weakened monsoon rainfall, with a corresponding rise in atmospheric CO_2 (33), followed by an abrupt warming over Greenland, strengthening of the monsoon, and sharp rise in atmospheric CH_4 (25). Pink boxes indicate terminal Northern Hemisphere cold periods. Red and blue dots are predicted D-O warming events using a fixed or variable threshold, respectively. Lowermost curves in each panel are moving windows of the standard deviation of AA_{T_hi} , our “bipolar seesaw activity index” (note that orbital time scale variations have been removed; blue is 5000-year window; green is 10,000-year window). Increased millennial-scale activity is generally observed during transitions between climate states, with minimal activity during interglacials and glacial maxima. All records are on the new Speleo-Age (A) or the EDC3 (B) time scale except the benthic $\delta^{18}O$ stack (LR04) of (34), which is on its own time scale.



alternative to the ultimate dependence on orbital tuning. In addition to providing an absolute time scale for the ice and gas records from Antarctica, we can also use our absolutely dated Greenland reconstruction as a tuning target for other high-resolution paleo-records, such as records of ice-rafted debris (IRD) from a North Atlantic sediment core (4) and a record of sea surface temperature (SST) from a core off the Iberian Margin (27) (Fig. 4). Each of these records has been tuned to our reconstruction on its absolute time scale (6).

Our synthetic records confirm that millennial time scale variability and abrupt climate oscillations occurred in Greenland throughout the past 800,000 years, and more specifically they suggest that the underlying physical mechanisms represented by the conceptual thermal bipolar seesaw were relatively invariant throughout this period. In line with observations for the last glacial period (28), our reconstructions suggest that higher-amplitude variability and more frequent D-O-like warming events occurred when climate was in an intermediate state or during the transitions between states (Fig. 4). Extending the observations of (22), we find that glacial terminations of the Middle to Late Pleistocene in general were characterized by oscillations of the bipolar seesaw.

This apparently ubiquitous association of millennial-scale climate variability with glacial terminations raises an important question: Is this mode of variability a necessary component of deglacial climate change, or merely a complicating factor? Previous studies (28, 29) have suggested that D-O-type variability might represent an inherent resonance of the climate system, attaining a high amplitude only within certain windows of opportunity (i.e., intermediate climate states). Given that global climate must pass through such

a window during deglaciation, one could argue that terminal oscillations of the bipolar seesaw are merely a symptom of deglacial climate change (29). However, the precise correspondence observed between bipolar seesaw oscillations and changes in atmospheric CO₂ during glacial terminations (Fig. 4) suggests that the bipolar seesaw may play more than just a passive role in the mechanism of deglaciation (i.e., through the positive feedbacks associated with increasing CO₂) (14, 19, 22). With the supercritical size of continental ice sheets as a possible precondition (30), and in combination with the right insolation forcing (31) and ice albedo feedbacks, the CO₂ rise associated with an oscillation of the bipolar seesaw could provide the necessary additional forcing to promote deglaciation. In this sense, the overall mechanism of glacial termination during the Middle to Late Pleistocene might be viewed as the timely and necessary interaction between millennial and orbital time scale variations.

References and Notes

1. W. Dansgaard *et al.*, *Science* **218**, 1273 (1982).
2. M. Stuiver, P. M. Grootes, *Quat. Res.* **53**, 277 (2000).
3. G. Bond *et al.*, *Nature* **365**, 143 (1993).
4. J. F. McManus, D. W. Oppo, J. L. Cullen, *Science* **283**, 971 (1999).
5. Y. J. Wang *et al.*, *Nature* **451**, 1090 (2008).
6. See supporting material on Science Online.
7. J. Jouzel *et al.*, *Science* **317**, 793 (2007).
8. W. S. Broecker, *Paleoceanography* **13**, 119 (1998).
9. T. F. Stocker, S. J. Johnsen, *Paleoceanography* **18**, 1087 (2003).
10. K. E. Trenberth, J. M. Caron, *J. Clim.* **14**, 3433 (2001).
11. M. Vellinga, R. A. Wood, *Clim. Change* **54**, 251 (2002).
12. J. C. H. Chiang, M. Biasutti, D. S. Battisti, *Paleoceanography* **18**, 1094 (2003).
13. R. F. Anderson *et al.*, *Science* **323**, 1443 (2009).
14. S. Barker *et al.*, *Nature* **457**, 1097 (2009).

15. A. Schmittner, O. A. Saenko, A. J. Weaver, *Quat. Sci. Rev.* **22**, 659 (2003).
16. E. J. Steig, R. B. Alley, *Ann. Glaciol.* **35**, 451 (2002).
17. T. Blunier, E. J. Brook, *Science* **291**, 109 (2001).
18. M. Siddall *et al.*, *Quat. Sci. Rev.* **25**, 3185 (2006).
19. E. W. Wolff, H. Fischer, R. Rothlisberger, *Nat. Geosci.* **2**, 206 (2009).
20. E. Capron *et al.*, *Quat. Sci. Rev.* **29**, 222 (2010).
21. E. Capron *et al.*, *Clim. Past* **6**, 345 (2010).
22. H. Cheng *et al.*, *Science* **326**, 248 (2009).
23. V. Margari *et al.*, *Nat. Geosci.* **3**, 127 (2010).
24. N. J. Shackleton, M. A. Hall, E. Vincent, *Paleoceanography* **15**, 565 (2000).
25. L. Loulergue *et al.*, *Nature* **453**, 383 (2008).
26. F. Parrenin *et al.*, *Clim. Past* **3**, 485 (2007).
27. B. Martrat *et al.*, *Science* **317**, 502 (2007).
28. M. Schulz, W. H. Berger, M. Samthein, P. M. Grootes, *Geophys. Res. Lett.* **26**, 3385 (1999).
29. A. Sima, A. Paul, M. Schulz, *Earth Planet. Sci. Lett.* **222**, 741 (2004).
30. M. E. Raymo, *Paleoceanography* **12**, 577 (1997).
31. J. D. Hays, J. Imbrie, N. J. Shackleton, *Science* **194**, 1121 (1976).
32. M. F. Sánchez Goñi, F. Eynaud, J. L. Turon, N. J. Shackleton, *Earth Planet. Sci. Lett.* **171**, 123 (1999).
33. D. Lüthi *et al.*, *Nature* **453**, 379 (2008).
34. L. E. Lisiecki, M. E. Raymo, *Paleoceanography* **20**, PA1003 (2005).

Acknowledgments: We thank the authors of all of the studies cited here for making their results available for this work. Supported by a Philip Leverhulme Prize (S.B.), Natural Environment Research Council (UK) awards NE/F002734/1 and NE/G004021/1 (S.B.), and NSF grants 0502535 and 1103403 (R.L.E.). This study is also part of the British Antarctic Survey Polar Science for Planet Earth Programme, funded by the Natural Environment Research Council (UK).

Supporting Online Material

www.sciencemag.org/cgi/content/full/science.1203580/DC1
Materials and Methods
Figs. S1 to S14
Tables S1 to S3
References

31 January 2011; accepted 26 August 2011
Published online 8 September 2011;
10.1126/science.1203580

Pre-Clovis Mastodon Hunting 13,800 Years Ago at the Manis Site, Washington

Michael R. Waters,^{1*} Thomas W. Stafford Jr.,^{2,5} H. Gregory McDonald,³ Carl Gustafson,⁴ Morten Rasmussen,⁵ Enrico Cappellini,⁵ Jesper V. Olsen,⁶ Damian Szklarczyk,⁶ Lars Juhl Jensen,⁶ M. Thomas P. Gilbert,⁵ Eske Willerslev⁵

The tip of a projectile point made of mastodon bone is embedded in a rib of a single disarticulated mastodon at the Manis site in the state of Washington. Radiocarbon dating and DNA analysis show that the rib is associated with the other remains and dates to 13,800 years ago. Thus, osseous projectile points, common to the Beringian Upper Paleolithic and Clovis, were made and used during pre-Clovis times in North America. The Manis site, combined with evidence of mammoth hunting at sites in Wisconsin, provides evidence that people were hunting proboscideans at least two millennia before Clovis.

Recent studies have strengthened the case that the makers of Clovis projectile points were not the first people to occupy the Americas (1–5). If hunting by humans was responsible for the megafauna extinction at the

end of the Pleistocene (6), hunting pressures must have begun millennia before Clovis (7). Here we reexamine the evidence from the Manis site in the state of Washington (8), an early mastodon kill that dates to 800 years before Clovis.

Between 1977 and 1979, a single male mastodon (*Mammuth americanum*) was excavated from sediments at the base of a kettle pond at the Manis site (figs. S1 to S3) (8–10). Some bones were spirally fractured, multiple flakes were removed from one long bone fragment, and other bones showed cut marks (8, 11, 12). The only documented artifact associated with the mastodon was a foreign osseous fragment, interpreted as the tip of a bone or antler projectile point,

¹Center for the Study of the First Americans, Departments of Anthropology and Geography, Texas A&M University, 4352 TAMU, College Station, TX 77843–4352, USA. ²Stafford Research, 200 Acadia Avenue, Lafayette, CO 80026–1845, USA. ³Park Museum Management Program, National Park Service, 1201 Oakridge Drive, Suite 150, Fort Collins, CO 80525, USA. ⁴245 Southeast Derby Street, Pullman, WA 99163–2217, USA. ⁵Centre for GeoGenetics, University of Copenhagen, Øster Voldgade 5–7, 1350 Copenhagen, Denmark, ⁶Novo Nordisk Foundation Center for Protein Research, Faculty of Health Sciences, University of Copenhagen, Blegdamsvej 3b, 2200 Copenhagen, Denmark.

*To whom correspondence should be addressed. E-mail: mwaters@tamu.edu